Interaction of an extended series of *N*-substituted di(2-picolyl)amine derivatives with copper(II). Synthetic, structural, magnetic and solution studies†

Bianca Antonioli,[a] Bernd Büchner,[b] Jack K. Clegg,[c] Kerstin Gloe,[a] Karsten Gloe,*[a] Linda Götzke,[a] Axel Heine,[a] Anne Jäger,[a] Katrina A. Jolliffe,[c] Olga Kataeva,[b,d] Vladislav Kataev,[b] Rüdiger Klingeler,[b] Tilo Krause,[a] Leonard F. Lindoy,*[c] Andreia Popa,[b] Wilhelm Seichter[e] and Marco Wenzel[a]

Received 28th January 2009, Accepted 30th March 2009
First published as an Advance Article on the web 29th April 2009
DOI: 10.1039/b901832h

The interaction of Cu(II) with the following secondary *N*-substituted derivatives of di(2-picolyl)amine (**1**) are reported: *N*-cyclohexylmethyl-di(2-picolyl)amine (**2**), *N*-benzyl-di(2-picolyl)amine (**3**), *N*-(4-pyridylmethyl)-di(2-picolyl)amine (**4**), *N*-(4-carboxymethylbenzyl)-di(2-picolyl)amine (**5**), *N*-(9-anthracen-8-ylmethyl)-di(2-picolyl)amine (**6**), 1,3-bis[di(2-picolyl)aminomethyl]benzene (**7**), 1,4-bis[di(2-picolyl)aminomethyl]benzene (**8**) and 2,4,6-tris[di(2-picolyl)amino]triazine (**9**). The solid complexes [Cu(**2**)(μ-Cl)]$_2$(PF$_6$)$_2$, [Cu(**3**)(μ-Cl)]$_2$(PF$_6$)$_2$·0.5CH$_2$Cl$_2$, Cu(**4**)(ClO$_4$)$_2$, Cu(**5**)$_2$(ClO$_4$)$_2$, [Cu(**6**)(ClO$_4$)$_2$(H$_2$O)]·0.5H$_2$O, Cu$_2$(**7**)(ClO$_4$)$_4$, [Cu$_2$(**8**)(Cl)$_4$] and [Cu$_2$(**9**+H)(μ-OCH$_3$)$_2$(H$_2$O)](ClO$_4$)$_3$·C$_4$H$_{10}$O were isolated and X-ray structures of [Cu(**2**)(μ-Cl)]$_2$(PF$_6$)$_2$, [Cu(**3**)(μ-Cl)]$_2$(PF$_6$)$_2$·0.5CH$_2$Cl$_2$, [Cu(**6**)$_2$(ClO$_4$)$_2$(H$_2$O)]·0.5H$_2$O, [Cu$_2$(**8**)Cl$_4$] and [Cu$_2$(**9**+H)(μ-OCH$_3$)$_2$(H$_2$O)](ClO$_4$)$_3$·C$_4$H$_{10}$O were obtained. The series is characterised by a varied range of coordination geometries and lattice architectures which in the case of [Cu(**6**)(ClO$_4$)$_2$(H$_2$O)]·0.5H$_2$O includes a chain-like structure formed by unusual intermolecular π-interactions between metal bound perchlorate anions and the aromatic rings of adjacent anthracenyl groups. Variable temperature magnetic susceptibility measurements have been performed for [Cu(**2**)(μ-Cl)]$_2$(PF$_6$)$_2$ and [Cu(**3**)(μ-Cl)]$_2$(PF$_6$)$_2$·0.5H$_2$O over the range 2–300 K. Both compounds show Curie-Weiss behaviour, with the data indicating weak antiferromagnetic interaction between the pairs of copper ions in each complex. Liquid–liquid (H$_2$O/CHCl$_3$) extraction experiments involving **1–3** and **7–9** as extractants showed that, relative to the parent (unsubstituted) dipic ligand **1**, substitution at the secondary amine site in each case resulted in an increase in extraction efficiency towards Cu(II) (as its perchlorate salt); at least in part, this increase may be attributed to the enhanced lipophilicities of the *N*-substituted derivatives.

Introduction

The transition metal chemistry of polypyridyl ligands continues to receive much attention, in part reflecting their coordination versatility and the role that such systems often play in biological, catalytic, photoactive and sensor applications.[1] Di(2-picolyl)amine (dipic, **1**) and its secondary nitrogen substituted derivatives have been demonstrated to form strong complexes with a number of transition and post-transition metal ions. For example, several reports describe the interaction of the dipic moiety with Cu(II) to yield both mono- and bis-ligand derivatives whose solid state structures have been reported in several instances.[2–13]

The interaction of Cu(II) with dipic derivatives incorporating substitution at the secondary nitrogen centre (including linked di- and tri-dipic derivatives) has also been investigated although individual systems of this type have received less attention than those of dipic itself.[2,14–30] Nevertheless, a number of copper derivatives of dipic and its substituted derivatives have been demonstrated to be effective reagents for the interaction with and oxidative cleavage of DNA.[15,31–33] We now report the results of an investigation aimed at extending the Cu(II) chemistry of both the parent dipic ligand **1** and its *N*-substituted derivatives **2–9**. With respect to this, it is noted that we have recently reported the results of an investigation of the complexation behaviour of a related series of *N*-substituted derivatives of 2,2′-dipyridylamine (dpa) with Cu(II),[34] Pd(II)[34] and Ag(I).[35] Unlike dipic and its derivatives of the above type, which usually bind to a metal *via* all three nitrogen donors of each dipic domain present, the dpa derivatives only employ the two pyridyl nitrogens from each dpa domain for such binding - that is, the aliphatic amine site remains uncoordinated. Hence, as already observed in previous studies, a significant difference in coordination behaviour is expected

[a]*Department of Chemistry and Food Chemistry, Technical University Dresden, 01062, Dresden, Germany*
[b]*IFW Dresden, P.O.B. 270116, 01171, Dresden, Germany*
[c]*School of Chemistry, University of Sydney, NSW 2006, Australia*
[d]*A. E. Arbuzov Institute of Organic and Physical Chemistry, Kazan, 420088, Russia*
[e]*Institute of Organic Chemistry, Technical University Freiberg, 09596, Freiberg, Germany*

† Electronic supplementary information (ESI) available: Additional crystallographic parameters and ORTEP diagrams. CCDC reference numbers 718366–718370. For ESI and crystallographic data in CIF or other electronic format see DOI: 10.1039/b901832h

between corresponding ligands belonging to the dpa and dipic derivative ligand categories.

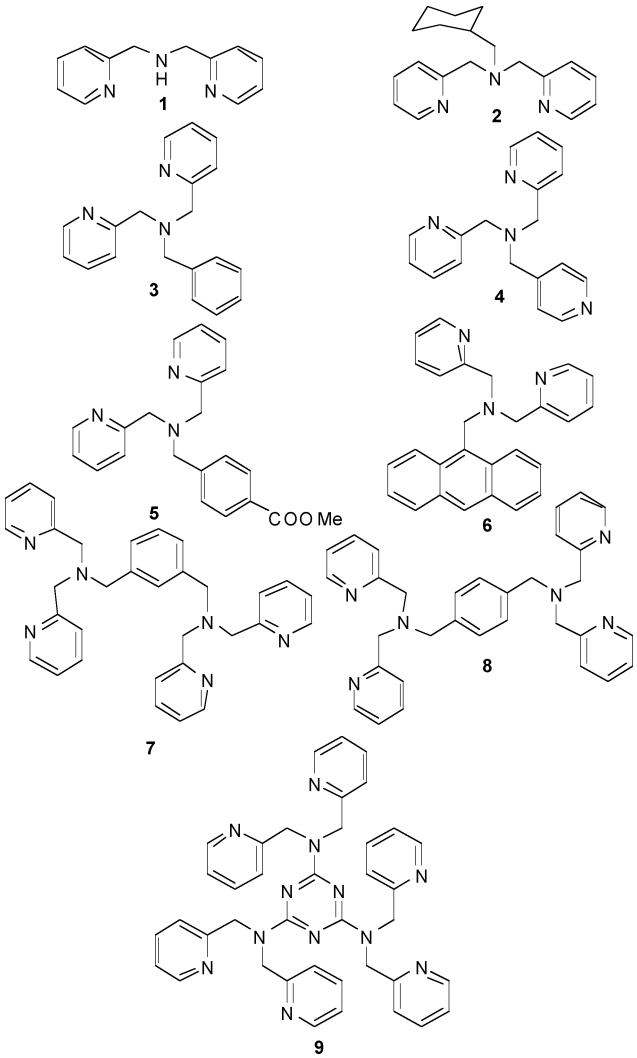

Experimental

Physical methods

NMR spectra were determined on a DRX-500 Bruker or Varian 300 MHz spectrometer. Column chromatography was performed on silica gel 60 (0.040–0.063 mm Merck) or neutral Al_2O_3 (FH 300 mm, HNS 29 Por.0). Melting points are uncorrected. ESI-MS were determined on a Micromass LCT-TOF mass spectrometer. Static magnetic susceptibility was measured with a Superconducting Quantum Interference Device (SQUID) Magnetometer from Quantum Design. The ESR measurements were performed with an X-Band (10 GHz) Bruker EMX Spectrometer.

Ligand synthesis

Di(2-picolyl)amine (**1**) used for preparation of the *N*-substituted derivatives was obtained commercially. Ligands **2** and **4** are new and were prepared as described below. Ligands **3**,[21] **5**,[36] **6**,[37] **7**,[38] **8**[38] and **9**[40] were prepared as described previously.

***N*-Cyclohexylmethyl-di(2-picolyl)amine (2).** A few crystals of KI were added to di(2-picolyl)amine (0.70 g, 3.52 mmol) and K_2CO_3 (0.97 g, 7.03 mol) suspended in acetone (10 mL) and bromomethylcyclohexane (0.62 g, 3.52 mol) in acetone (20 mL) was added dropwise over 30 min. The mixture was heated at reflux for 24 h, the acetone was then removed under vacuum, and the residue was dissolved in $CHCl_3$ (100 mL). This solution was washed twice with water (100 mL) then the organic phase was dried over $MgSO_4$, filtered, and the solvent removed under vacuum. The residue was purified by column chromatography [$CHCl_3$/MeOH (98:2), SiO_2]. The desired product **2** was present in the first fraction as a brown oil. Yield: 0.6 g, (58%). $C_{19}H_{25}N_3$ (295.4) ESI-MS: m/z = 296 [M + H]$^+$. ^{1}H NMR (500 MHz, $CDCl_3$, 298 K): δ (ppm) = 1.07–1.84 (11H, m, cyclohexyl CH_2, CH), 2.30 (2H, d, NCH_2CH), 3.75 (4H, s, NCH_2Py), 7.11 (2H, t, *m*-PyH), 7.56 (2H, d, *m*-PyH), 7.63 (2H, t, *p*-PyH), 8.47 (2H, d, *o*-PyH). ^{13}C NMR (500 MHz, $CDCl_3$, 298 K): 26.0 (CH_2), 26.7 (CH_2), 31.6 (CH_2), 35.7 (CH), 60.9 (CH_2), 61.5 (CH_2), 121.8 (CH), 122.8 (CH), 136.4 (CH), 148.8 (CH), 160.0 (Cq).

***N*-Benzyl-di(2-picolyl)amine (3)[21].** Yield: 10%, brown oil. $C_{19}H_{19}N_3$ (289.4) ESI-MS: m/z = 290 [M + H]$^+$. ^{1}H NMR (500 MHz, $CDCl_3$, 298 K): δ (ppm) = 3.74 (2H, d, CH_2Ph), 3.86 (4H, s, CH_2Py), 7.11 (5H, m, Ph), 7.13 (2H, t, *m*-PyH), 7.56 (2H, d, *m*-PyH), 7.66 (2H, t, *p*-PyH), 8.50 (2H, d, *o*-PyH). ^{13}C NMR (500 MHz, $CDCl_3$, 298 K): δ (ppm) = 56.0 (CH_2), 60.0 (CH_2), 122.3 (CH), 122.82 (CH), 127.0 (Cq), 128.38 (CH), 128.91(CH), 136.0 (CH), 139.1 (CH), 150.0 (CH), 159.7 (Cq).

***N*-(4-Pyridylmethyl)-di(2-picolyl)amine (4).** To 4-chloromethylpyridine hydrochloride (1.64 g, 10.0 mmol) suspended in acetone (15 mL) was added NaOH (0.400 g, 10.0 mmol) in water (10 mL). When the 4-chloromethylpyridine hydrochloride had dissolved, the resulting yellow solution was added dropwise to a mixture of di(2-picolyl)amine (1.395 g, 7.00 mmol) and K_2CO_3 (0.97 g, 7.00 mmol) in acetone (40 mL) and the solution was heated at reflux for 6 h. The solvent was removed under vacuum and the residue was shaken with a 1:1 mixture of water and chloroform. The aqueous phase was separated and washed three times with chloroform; the organic phases were combined then washed three times with water. The organic phase was dried over $MgSO_4$, filtered, and the solvent removed under vacuum. A brown oil remained that was purified by column chromatography (ethyl acetate, SiO_2). Yield: 1.03 g (51%). $C_{18}H_{18}N_4$ (290.4) ESI-MS: m/z = 291 [M + H]$^+$. ^{1}H NMR (500 MHz, $CDCl_3$, 298 K): δ (ppm) = 3.70 (2H, s, CH_2Py); 3.80 (4H, s, CH_2Py); 7.15 (2H, t, PyH); 7.34 (2H, d, PyH); 7.52 (2H, d, PyH); 7.66 (2H, t, PyH); 8.51 (4H, m, PyH). ^{13}C NMR (500 MHz, $CDCl_3$, 298 K): 57.3 (CH_2); 60.1 (CH_2); 122.2 (CH); 122.8 (CH); 123.7 (CH);136.6 (CH); 148.5 (Cq); 149.1 (CH); 158.9 (Cq).

***N*-(4-Carboxymethylbenzyl)-di(2-picolyl)amine (5)[36].** Yield: 70%, yellow oil. $C_{21}H_{21}N_3O_2$ (347.4) ESI-MS: m/z = 348 [M + H]$^+$. ^{1}H NMR (500 MHz, $CDCl_3$, 300 K): δ (ppm) = 3.89 (3H, s, OCH_3); 4.10 (2H, s, br, CH_2Ar); 4.19 (4H, s, br, CH_2Py); 7.31 (2H, t, *m*-PyH); 7.58 (2H, d, ArH); 7.71 (2H, d, *m*-PyH); 7.80 (2H, t, *p*-PyH); 7.97 (2H, d, ArH); 8.59 (2H, d, *o*-PyH).

***N*-(9-Anthracen-8-ylmethyl)-di(2-picolyl)amine (6)[37].** Yield: 64%, yellow crystals. $C_{27}H_{23}N_3$ (389.5) ESI-MS: m/z = 390

$[M + H]^+$. ^1H NMR (500 MHz, $CDCl_3$, 300 K): δ (ppm) = 4.07 (4H, s, br, CH_2Py); 4.81 (2H, s, br, CH_2Ar); 7.13 (2H, t, *m*-PyH); 7.28 (2H, d, *m*-PyH); 7.44 (2H, t, ArH); 7.51 (2H, t, ArH); 7.58 (2H, t, *p*-PyH); 7.93 (2H, d, ArH); 8.34 (1H, s, ArH); 8.43 (2H, d, ArH); 8.47 (2H, d, *o*-PyH).

1,3-Bis[di(2-picolyl)aminomethyl]benzene (7)[38]. Yield: 94%, brown oil. $C_{32}H_{32}N_6$ (500.6) ESI-MS: m/z = 501 $[M + H]^+$. ^1H NMR (500 MHz, $CDCl_3$, 300 K): δ (ppm) = 3.79 (4H, s, br, CH_2Ar); 3.90 (8H, s, br, CH_2Py); 7.15 (4H, t, *m*-PyH); 7.28 (1H, d, ArH); 7.33 (2H, d, ArH); 7.52 (1H, s, ArH); 7.63 (8H, m, *m*-PyH, *p*-PyH); 8.51 (4H, d, *o*-PyH).

1,4-Bis[di(2-picolyl)aminomethyl]benzene (8)[38]. Yield: 64%, brown oil. $C_{32}H_{32}N_6$ (500.6) ESI-MS: m/z = 501 $[M + H]^+$. ^1H NMR (500 MHz, $CDCl_3$, 300 K): δ (ppm) = 3.98 (4H, s, br, CH_2Ar); 4.08 (8H, s, br, CH_2Py); 7.21 (4H, t, *m*-PyH); 7.46 (4H, s, ArH); 7.65 (4H, d, *m*-PyH); 7.71 (4H, t, *p*-PyH); 8.54 (4H, d, *o*-PyH).

2,4,6-Tris[di(2-picolyl)amino]triazine (9)[39]. Yield: 58%, white solid. $C_{39}H_{36}N_{12}$ (672.8) ESI-MS: m/z = 673 $[M + H]^+$. ^1H NMR (500 MHz, $CDCl_3$, 300 K): δ (ppm) = 4.26 (6H, s, br, N^+–H); 4.88 (12H, s, CH_2Py); 7.09 (6H, d, *m*-PyH); 7.15 (6H, t, *m*-PyH); 7.53 (6H, t, *p*-PyH); 8.62 (6H, d, *o*-PyH).

Complex synthesis

Perchlorate complexes are potentially explosive and appropriate caution should be exercised in their synthesis and handling.

$[Cu(2)(\mu\text{-}Cl)]_2(PF_6)_2$. $CuCl_2{\cdot}2H_2O$ (0.05 g, 0.29 mmol) in ethanol (10 mL) was added to a stirred solution of **2** (0.086 g, 0.29 mmol) in dichloromethane (10 mL). To this solution was added NH_4PF_6 (0.24 g, 1.5 mmol) in ethanol (3 mL). Diethyl ether vapour diffusion into this solution led to formation of blue crystals which were isolated, washed with diethyl ether and allowed to dry in air. Yield: 0.219 g (75%). Found: C, 42.16; H, 4.66; N, 7.59. Calcd. for $C_{38}H_{50}Cl_2Cu_2F_{12}N_6P_2$: C, 42.31; H, 4.67; N, 7.79%.

$[Cu(3)(\mu\text{-}Cl)]_2(PF_6)_2{\cdot}0.5CH_2Cl_2$. This was obtained as blue crystals by an identical procedure to that described above for $[Cu(\mathbf{2})(\mu\text{-}Cl)]_2(PF_6)_2$. Yield: 0.027 g (86%). Found: C, 42.43; H, 3.65; N, 7.81. Calcd. for $C_{38}H_{38}Cl_2Cu_2F_{12}N_6P_2$: C, 42.79; H, 3.59; N, 7.88%. ESI-MS: m/z 811 $[2Cu + 2L + 3Cl]^+$. Portion of the above product was recrystallised from dichloromethane, an X-ray structure determination on this product showed it to have the composition $[Cu(\mathbf{3})(\mu\text{-}Cl)]_2(PF_6)_2{\cdot}0.5CH_2Cl_2$.

$Cu(4)(ClO_4)_2$. $Cu(ClO_4)_2{\cdot}6H_2O$ (0.031 g, 0.083 mmol) in methanol (1 mL) was added to **4** (0.024 g, 0.083 mmol) in methanol (2 mL). Diffusion of diethyl ether vapor into this solution resulted in a blue precipitate that was isolated, washed with ether, and allowed to dry in air. Yield: 0.026 g (57%). Found: C, 38.78; H, 3.20; N, 9.95. Calcd. for $C_{18}H_{18}Cl_2CuN_4O_8$: C 39.11; H 3.28; N 10.13%.

$Cu(5)_2(ClO_4)_2$. $Cu(ClO_4)_2{\cdot}6H_2O$ (0.009 g, 0.023 mmol) in methanol (1 mL) was added to a solution of **5** (0.016 g, 0.046 mmol) in methanol (2 mL). Diffusion of diethyl ether vapour into this solution resulted in a green crystalline product which was isolated, washed with ether, and allowed to dry in air. Yield: 0.009 g (43%). Found: C, 53.02; H, 4.49; N, 9.15. Calcd. for $C_{42}H_{42}Cl_2CuN_6O_{12}$: C, 52.70; H, 4.42; N, 8.78%.

$[Cu(6)(ClO_4)_2(H_2O)]$. $Cu(ClO_4)_2{\cdot}6H_2O$ (0.033 g, 0.090 mmol) in methanol (1 mL) was added to **6** (0.035 g, 0.090 mmol) in methanol (2 mL). Diffusion of diethyl ether vapour into this intense green solution resulted in a dark green crystalline product which was isolated, washed with ether, and allowed to dry in air. Yield: 0.039 g (64%). Found: C, 47.92; H, 3.76; N, 6.26. Calcd. for $C_{27}H_{25}Cl_2CuN_3O_9$: C, 48.40; H, 3.76; N, 6.27%. An X-ray structure determination on this product taken directly from the reaction mixture showed it to have the composition $[Cu(\mathbf{6})(ClO_4)_2(H_2O)]{\cdot}0.5H_2O$.

$Cu_2(7)(ClO_4)_4$. $Cu(ClO_4)_2{\cdot}6H_2O$ (0.030 g, 0.080 mmol) in methanol (2 mL) was added to **7** (0.020 g, 0.040 mmol) in methanol (2 mL). The brown precipitate that initially formed was removed by filtration and diffusion of diethyl ether vapour into the green filtrate resulted in a blue-green crystalline product which was isolated, washed with ether and allowed to dry in air. Yield: 0.043 g (52%). Found: C, 37.80; H, 3.28; N, 8.62. Calcd. for $C_{32}H_{32}Cl_4Cu_2N_6O_{16}$: C, 37.48; H, 3.15; N, 8.19%.

$[Cu_2(8)Cl_4]$. A solution of **8** (0.025 g, 0.049 mmol) in dichloromethane (2 mL) was carefully overlaid with a solution of $CuCl_2{\cdot}2H_2O$ (0.017 g, 0.099 mmol) in ethanol (2 mL). Blue crystals formed within two days following diethyl ether vapour diffusion. These were isolated, washed with diethyl ether and dried under vacuum. Yield: 0.026 (69%). Found: C, 49.75; H, 4.15; N, 10.90. Calcd. for $C_{32}H_{32}Cl_4Cu_2N_6$: C, 49.94; H, 4.19; N, 10.92%. ESI-MS, m/z = 733 $[L + 2Cu + 3Cl]^+$.

$[Cu_2(9+H)(\mu\text{-}OCH_3)_2(H_2O)](ClO_4)_3{\cdot}2H_2O$. A solution of **9** (0.033 g, 0.049 mmol) in dichloromethane (5 mL) was overlaid carefully with a solution of $CuCl_2{\cdot}2H_2O$ (0.054 g, 0.15 mmol) in methanol (5 mL). Blue-green crystals formed over one week following diethyl ether vapour diffusion into the solution. These were isolated, washed with diethyl ether and allowed to dry in air. Yield: 0.045 (76%). Found: C, 40.55; H, 3.98; N, 13.84. Calcd. for $C_{41}H_{43}Cl_3Cu_2N_{12}O_{14}{\cdot}3H_2O$: C, 40.52; H, 4.06; N, 13.82%.

Solvent extraction experiments

Liquid–liquid extraction experiments were performed at 23 ± 1 °C in microcentrifuge tubes (2 cm^3) with a phase ratio $V_{(org)}:V_{(aq)}$ of 1:1 (500 μL each). The aqueous phase contained $Cu(ClO_4)_2$ (1×10^{-4} M), sodium perchlorate (5×10^{-3} M) as supporting anion and the zwitterionic buffer system, HEPES/NaOH, at pH 7.2; as a precaution, the pH of the aqueous phase was monitored before and after each experiment with the aid of an InLab423 pH electrode. The organic phase contained a known concentration of ligand in chloroform (1×10^{-3} M). All experiments involved the mechanical shaking of the two-phase system for 30 min (T = 23 ± 1 °C) by which time equilibrium was reached (as established by preliminary experiments). At the end of this time, the phases were separated, centrifuged and the depletion of the metal ion concentrations in the aqueous phase was measured using an ICP-MS (ELAN 9000/Perkin Elmer) spectrometer.

Table 1 Crystal data for the Cu(II) complexes of **2**, **3**, **6**, **8** and **9**

Compound	[Cu(**2**)(μ-Cl)]$_2$(PF$_6$)$_2$	[Cu(**3**)(μ-Cl)]$_2$(PF$_6$)$_2$·0.5CH$_2$Cl$_2$	[Cu(**6**)(ClO$_4$)$_2$(H$_2$O)]·0.5H$_2$O	[Cu$_2$(**8**)Cl$_4$]	[Cu$_2$(**9**+H)(μ-OCH$_3$)$_2$(H$_2$O)](ClO$_4$)$_3$·C$_4$H$_{10}$O
Formula of refinement model	$C_{38}H_{30}Cl_2Cu_2F_{12}N_6P_2$	$C_{77}H_{78}C_{16}Cu_4F_{24}N_{12}P_4$	$C_{54}H_{52}Cl_4Cu_2N_6O_{19}$	$C_{32}H_{32}Cl_4Cu_2N_6$	$C_{45}H_{55}Cl_3Cu_2N_{12}O_{16}$
Molecular weight	1078.76	2218.29	1357.90	769.52	1253.44
Crystal system	Monoclinic	Monoclinic	Monoclinic	Monoclinic	Monoclinic
Space group	*C*2/*c*(#15)	*P*21/*n*(#14)	*P*21/*n*(#14)	*P*21/*n*(#14)	*P*21/*c*(#14)
a/Å	25.992(5)	13.347(2)	14.1257(3)	8.702(1)	14.266(3)
b/Å	7.118(1)	14.191(2)	10.5924(2)	12.422(1)	23.434(4)
c/Å	26.973(5)	14.720(2)	36.7101(6)	14.911(2)	15.982(5)
β/°	112.76(3)	115.575(17)	99.343(1)	90.17(1)	98.86(2)
V/Å^3	4601.7(17)	2514.9(7)	5419.88(18)	1611.9(3)	5279(2)
D_c/g cm^{-3}	1.557	1.465	1.664	1.585	1.577
Z	4	1	4	2	4
Crystal size/mm	0.49 × 0.42 × 0.33	0.15 × 0.13 × 0.09	0.30 × 0.28 × 0.20	0.17 × 0.14 × 0.10	0.25 × 0.25 × 0.17
Crystal colour	blue	green	blue	green	blue
Crystal habit	block	prism	prism	block	irregular
Temperature/K	293(2)	293(2)	150(2)	198(2)	198(2)
μ(MoKα)/mm^{-1}	1.194	1.147	1.067	1.685	1.038
T(SADABS)$_{min,max}$	0.56474, 0.67318	0.810, 0.902	0.711, 0.808	0.7627, 0.8496	0.723, 0.843
$2\theta_{max}$/°	60.00	45.00	63.12	61.02	50.80
hkl range	−35 36, −9 10, −37 37	−14 14, −15 15, −15 15	−13 20, −15 15, −44 54	−12 12, −17 17, −21 21	−17 17, −28 28, −19 19
N	39746	18022	118862	37856	169744
N_{ind} (R_{merge})	6667 (0.0300)	3139 (0.1935)	17776 (0.0734)	4935 (0.0387)	9704 (0.0566)
N_{obs} ($I > 2\sigma(I)$)	4915	1597	9736	3785	7957
*R*1[a] ($I > 2\sigma(I)$), *wR*2[a] (all)	0.0468, 0.1385	0.0877, 0.2584	0.0475, 0.0964	0.0369, 0.0891	0.0638, 0.1647
A[a], *B*[a]	0.0671, 8.7751	0.1590, 0.0000	0.0256, 0.00000	0.0384, 1.2425	0.0536, 25.5575
GoF	1.043	0.938	1.110	1.027	1.105
Residual Extrema/e$^-$ Å^{-3}	−0.715, 0.734	−0.478, 0.880	−0.972, 2.169	0.499, 0.893	−1.327, 1.497

[a] $R1 = \sum||F_o| - |F_c||/\sum|F_o|$ for $F_o > 2\sigma(F_o)$ and $wR2 = \{\sum[w(F_o^2 - F_c^2)^2]/\sum[w(F_c^2)^2]\}^{1/2}$ where $w = 1/[\sigma^2(F_o^2) + (AP)^2 + BP]$, $P = (F_o^2 + 2F_c^2)/3$ and *A* and *B* are listed in the crystal data information supplied.

Crystallography†

Structures [Cu(**2**)(μ-Cl)]$_2$(PF$_6$)$_2$, [Cu(**3**)(μ-Cl)]$_2$(PF$_6$)$_2$·0.5CH$_2$Cl$_2$ and [Cu$_2$(**8**)Cl$_4$], were collected on a Nonius Kappa CCD with *ω* and *φ* scans at 198(2) or 293(2) K. Data collections were undertaken with COLLECT,[40] cell refinement with Dirax/lsq,[41] and data reduction with EvalCCD.[42] Structures [Cu(**6**)(ClO$_4$)$_2$(H$_2$O)]·0.5H$_2$O and [Cu$_2$(**9**+H)(μ-OCH$_3$)$_2$(H$_2$O)](ClO$_4$)$_3$·C$_4$H$_{10}$O were collected at 150(2) and 198(2) K respectively with a Bruker AXS Kappa APEX II CCD and SMART APEX II CCD diffractometers with *ω* and *φ* scans. Data integration and reduction were undertaken with SAINT and XPREP.[43] Each structure was solved by direct methods using SHELXS-97.[44] Both diffractometers employed graphite-monochromated Mo-Kα radiation generated from a sealed tube (0.71073 Å). Multi-scan empirical absorption corrections were applied to all data sets using the program SADABS.[45] All structures were refined and extended with SHELXL-97.[46] In general, ordered non-hydrogen atoms with occupancies greater than 0.5 were refined anisotropically. Partial occupancy carbon, nitrogen and oxygen atoms were refined isotropically, as were chlorine atoms with occupancy of 0.25 or less. Carbon-bound hydrogen atoms were included in idealised positions and refined using a riding model. Oxygen and nitrogen-bound hydrogen atoms that were structurally evident in the difference Fourier map were included and refined with bond length and angle restraints.

Crystal and structure refinement data for all structures are summarised in Table 1. Where applicable, further details relating to the X-ray structure refinements are given in the ESI† along with tables of bond lengths and angles for each structure together with selected H-bond and π-interaction geometries.

Results and discussion

Cu(II) complex synthesis

In an attempt to obtain suitable crystals for X-ray diffraction studies, the reaction of **2–9** with the appropriate Cu(II) salt under a variety of conditions resulted in isolation of the following new complexes: [Cu(**2**)(μ-Cl)]$_2$(PF$_6$)$_2$, [Cu(**3**)(μ-Cl)]$_2$(PF$_6$)$_2$·0.5CH$_2$Cl$_2$, Cu(**4**)(ClO$_4$)$_2$, Cu(**5**)$_2$(ClO$_4$)$_2$, [Cu(**6**)(ClO$_4$)$_2$(H$_2$O)]·0.5H$_2$O, Cu$_2$(**7**)(ClO$_4$)$_4$, [Cu$_2$(**8**)(Cl$_4$], and [Cu$_2$(**9**+H)(μ-OCH$_3$)$_2$(H$_2$O)](ClO$_4$)$_3$·C$_4$H$_{10}$O. Of these, [Cu(**2**)(μ-Cl)]$_2$(PF$_6$)$_2$, [Cu(**3**)(μ-Cl)]$_2$(PF$_6$)$_2$·0.5CH$_2$Cl$_2$, [Cu(**6**)(ClO$_4$)$_2$(H$_2$O)]·0.5H$_2$O, [Cu$_2$(**8**)Cl$_4$] and [Cu$_2$(**9**+H)(μ-OCH$_3$)$_2$(H$_2$O)](ClO$_4$)$_3$·C$_4$H$_{10}$O yielded suitable crystals for X-ray structure determination and the respective structures are discussed below.

Discussion of the X-ray structures

[Cu(2)(μ-Cl)]$_2$(PF$_6$)$_2$ and [Cu(3)(μ-Cl)]$_2$(PF$_6$)$_2$. Reaction of *N*-cyclohexylmethyl-di(2-picolyl)amine **2** in CH_2Cl_2 with $CuCl_2·2H_2O$ in ethanol in the presence of NH_4PF_6 yielded a blue crystalline complex. The X-ray structure (Fig. 1) of this product showed a μ-dichloro bridged dimer, disposed around an inversion centre, containing five-coordinate Cu(II) ions, with the latter separated by 3.50 Å; other selected bond lengths and angles are listed in Table S1 in the ESI.†

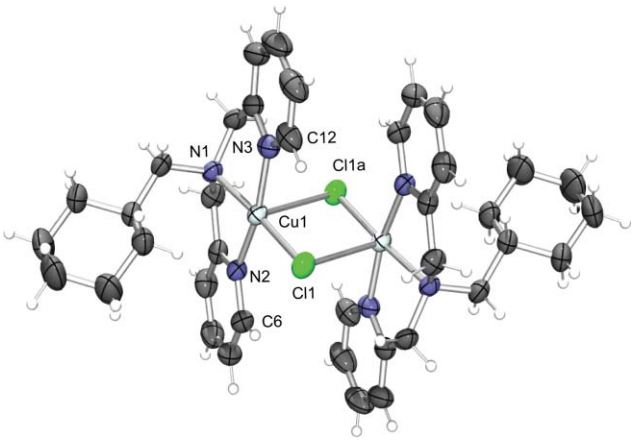

Fig. 1 ORTEP depiction of $[Cu(\mathbf{2})(\mu\text{-}Cl)]_2^{2+}$ showing selected atom labels (50% thermal ellipsoids).

The N_3Cl_2-coordination sphere of copper is best described as near square-pyramidal ($\tau = 0.14$).[47] The Cu1–N bond lengths involving the tertiary aliphatic N1 and heterocyclic nitrogen atoms N2 and N3 are similar at 2.002(2), 1.989(2) and 1.992(2) Å, respectively. The bridging 'equatorial' Cu–Cl bond lengths are 2.240(1) Å, contrasting with the longer 'axial' bridging Cu–Cl bond lengths of 2.929(1) Å.

Selected inter- and intramolecular interactions for $[Cu(\mathbf{2})(\mu\text{-}Cl)]_2(PF_6)_2$ are listed in Table 2. The dimeric arrangement is stabilised by intramolecular C–H···Cl interactions; Cl(1) is associated with two intramolecular C–H···Cl interactions with aryl C–H groups next to the pyridine-nitrogens C–H(6) and C–H(12) (Fig. 2). One PF_6^- [P(1)] counter ion is involved in a weak interaction with the complex cation [H(13A)···F(1A) = 2.36 Å; $-x, y, 1/2 - z$], with the corresponding C–H···F-distance being less than the sum of the van der Waals radii of 2.54 Å and comparable to literature values.[48,49]

Table 2 C–H···Cl and C–H···F interactions in $[Cu(\mathbf{2})(\mu\text{-}Cl)]_2(PF_6)_2$

C–H	A	C···H	H···A [Å]	C···A [Å]	C–H···A [°]
C(6)–H(6)	Cl(1)	0.93	2.77	3.314(4)	118
C(12)–H(12)	Cl(1)	0.93	2.77	3.310(3)	117
C(13)–H(13A)	F(1A)	0.97	2.52	3.277(6)	145
C(13)–H(13A)	F(1A)^{ia}	0.97	2.36	3.323(6)	161

[a] Symmetry transformation: (i) $-x, y, 1/2 - z$.

Similar experimental conditions to those employed for $[Cu(\mathbf{2})(\mu\text{-}Cl)]_2(PF_6)_2$ (but substituting *N*-benzyl-di(2-picolyl)amine **3** for **2**) yielded blue crystals formulated on the basis of its microanalysis and the presence of a peak in the ESI-MS at $m/z = 811$ (corresponding to a $[2Cu + 2L + 3Cl]^+$ ion) as a product of type $[Cu(\mathbf{3})(\mu\text{-}Cl)]_2(PF_6)_2 \cdot 0.5H_2O$ in which the benzyl substituent on the secondary nitrogen replaces the cyclohexylmethyl group in $[Cu(\mathbf{2})(\mu\text{-}Cl)]_2(PF_6)_2$. Recrystallisation of this product from dichloromethane gave crystals of stoichiometry $[Cu(\mathbf{3})(\mu\text{-}Cl)]_2(PF_6)_2 \cdot 0.5CH_2Cl_2$ suitable for an X-ray structure determination.

The resulting structure confirmed the presence of a dinuclear dichloro-bridged cation (Fig. 3) whose structure closely parallels that of the above complex of **2**. The charge on the complex cation is balanced by the presence of disordered PF_6^- anions in the lattice. A 3D-network results from an array of phenyl C–H to F (PF_6^-) and Cl (solvent) hydrogen bonds throughout the lattice.

It needs to be noted here that the structures of two closely related dinuclear dichloro-bridged complexes, $[Cu(\mathbf{3})(\mu\text{-}Cl)]_2(ClO_4)_2 \cdot 0.33CH_3OH$ and $[Cu(\mathbf{3})(\mu\text{-}Cl)]_2(ClO_4)_2 \cdot 0.67C_2H_5OH$, each incorporating the same complex cation as occurs in

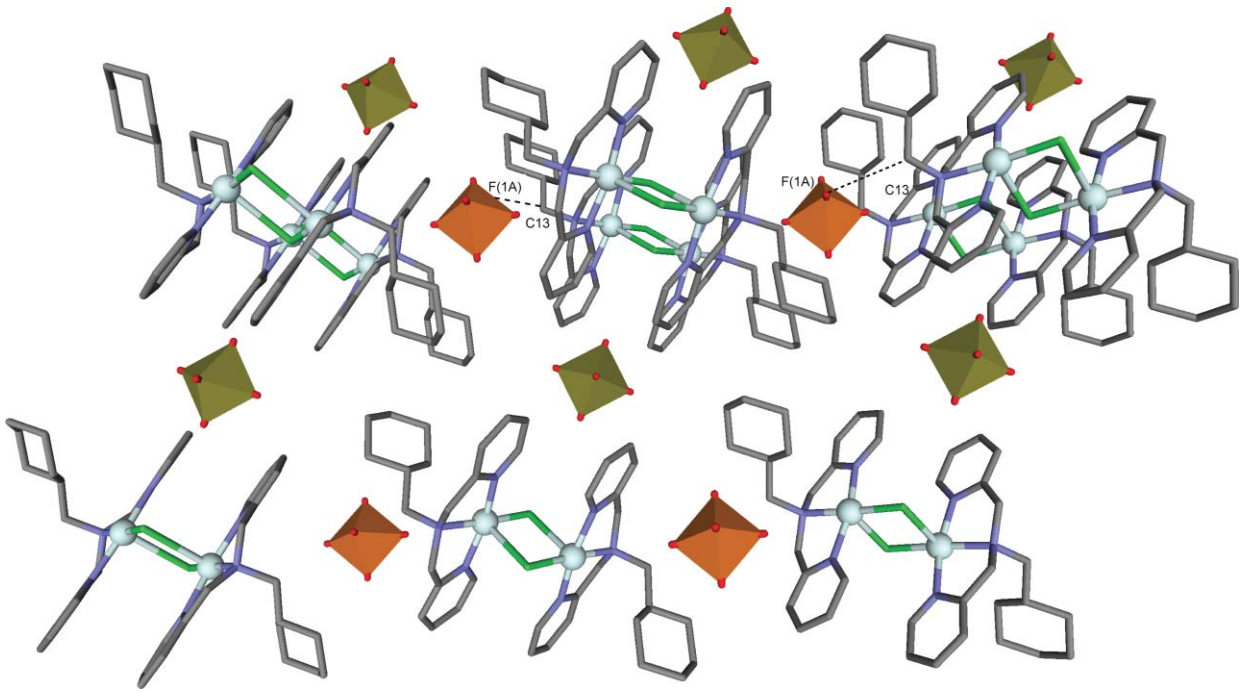

Fig. 2 Details of the crystal packing for $[Cu(\mathbf{2})(\mu\text{-}Cl)]_2(PF_6)_2$, showing the C–H···F interactions between PF_6^- and the complex cation $[Cu(\mathbf{2})(\mu\text{-}Cl)]_2^{2+}$ [C–H(13A)···F(1) = 3.32 Å; 161°, $-x, y, 1/2 - z$]; view along the *b*-axis.

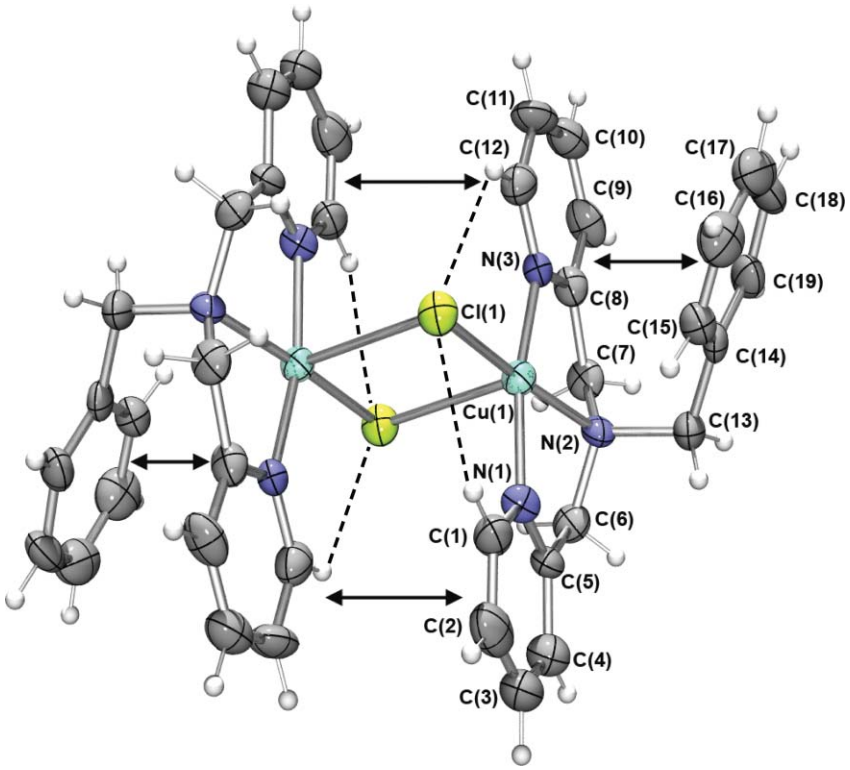

Fig. 3 Structure of the cation in $[Cu(\mathbf{3})(\mu\text{-}Cl)]_2(PF_6)_2\cdot 0.5CH_2Cl_2$ shown with 30% thermal ellipsoids; the symmetry code for equivalent atoms is $1-x, 1-y, -z$. Dashed lines indicate intramolecular pyridyl C–H···Cl hydrogen bonds and arrows indicate weak intramolecular offset face-to-face π–π interactions. The C(1)–C(12) separation is 3.36 Å and the centroid to centroid separation between the rings incorporating C(1) and C(15) is 3.75 Å.

$[Cu(\mathbf{3})(\mu\text{-}Cl)]_2(PF_6)_2\cdot 0.5CH_2Cl_2$ (but different anions), have been reported previously by Rojas *et al.*[21] and Kani *et al.*,[27] respectively. In both cases the cation geometries are similar to that in the present complex.

$[Cu(\mathbf{6})(ClO_4)_2(H_2O)]\cdot 0.5H_2O$. The structure determination of the anthracene-containing derivative, $[Cu(\mathbf{6})(ClO_4)_2(H_2O)]\cdot 0.5H_2O$ showed the presence of two molecules in the asymmetric unit (Fig. 4). Perhaps surprisingly given the presence of both anthracene and pyridyl moieties, the crystal packing is dominated by hydrogen bonding interactions, which give rise to a two-dimensional sheet-like motif (ESI, Table S4).† There are, however, some weak π interactions, the strongest of which is a perchlorate anion–π interaction[50] indicated by an O(4)–C(41)-containing centroid distance of 3.14 Å and a weaker anion–π interaction O(13)–C(14)-containing centroid of 3.47 Å to yield an

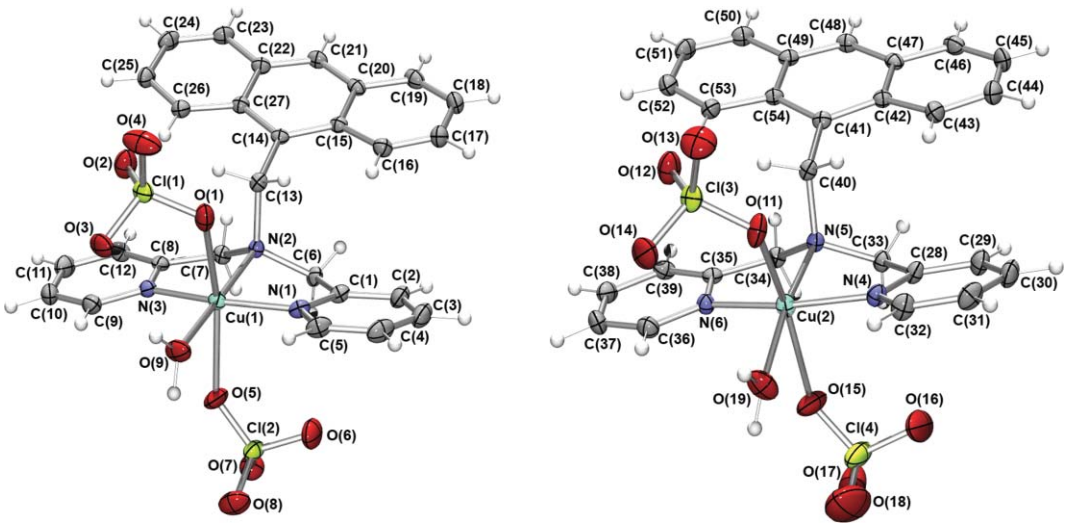

Fig. 4 X-Ray structure of $[Cu(\mathbf{6})(ClO_4)_2(H_2O)]\cdot 0.5H_2O$ showing the two independent molecules in the asymmetric unit, depicted with 50% thermal ellipsoids; solvate water molecules are not shown. Selected bond distances and angles are listed in the ESI (Table S3).†

overall one dimensional chain structure Fig. 5. There are also a number of weak offset face-to-face interactions of poor geometric orientation indicated by C(18)–C(10) separations of 3.51 Å and C(11)–C(31) of 3.75 Å.

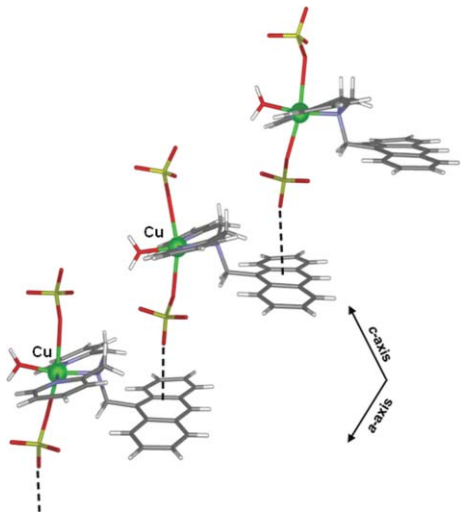

Fig. 5 The chain-like structure of $[Cu(\mathbf{6})(ClO_4)_2(H_2O)]\cdot 0.5H_2O$ formed by intermolecular π-interaction between bound perchlorate anions and the 'centre' aromatic rings of adjacent anthracenyl groups. Solvate water molecules not shown.

$[Cu_2(\mathbf{8})(Cl)_4]$. Reaction of 1,4-bis[di(2-picolyl)aminomethyl]benzene **8** in dichloromethane with $CuCl_2\cdot 2H_2O$ in ethanol in a 1:2 molar ratio yielded blue crystals. The microanalysis for this product coupled with the presence of a peak in its ESI mass spectrum at m/z 733 corresponding to $[2Cu + L + 3Cl]^+$ suggested that it was a dinuclear complex of type $[Cu_2(\mathbf{8})(Cl)_4]$. An X-ray diffraction study confirmed this stoichiometry. The complex crystallises in the monoclinic system and contains two molecules per unit cell. Each of the two di(2-picolyl)amine ligand subunits of **8** coordinate to a Cu(II) centre to yield the 2:1 (L:M) binuclear arrangement shown in Fig. 6. Each copper is bound to an N_3Cl_2 donor atom set, with the coordination geometry being square pyramidal ($\tau = 0.01$).[47]

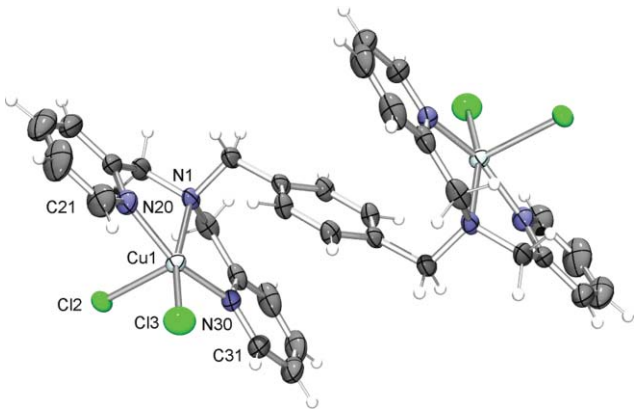

Fig. 6 ORTEP depiction of $[Cu_2(\mathbf{8})(Cl)_4]$ with selected atom labels (50% thermal ellipsoids).

Table 3 C–H···Cl interactions in $[Cu_2(\mathbf{8})(Cl)_4]$

C–H	A	C···H	H···A [Å]	C···A [Å]	C–H···A [°]
C(4)–H(4)	Cl(2)^{i}	0.95	2.66	3.586(4)	165
C(24)–H(24)	Cl(2)^{ii}	0.95	2.82	3.666(6)	149
C(21)–H(21)	Cl(3)	0.95	2.79	3.336(4)	117
C(31)–H(31)	Cl(3)	0.95	2.77	3.347(3)	120

[a] Symmetry transformation: (i) $3/2 - x, -1/2 + y, 1/2 - z$, (ii) $2 - x, -y, 1 - z$.

For Cu(1) the tertiary amine nitrogen N(1) together with the pyridine nitrogens N(20) and N(30) and the Cl(3) chloro ligand define the basal plane of the square pyramid while Cl(2) occupies the apical site. As commonly occurs in related complexes, the Cu(1) centre is positioned above (0.24 Å) the basal plane towards Cl(2). The Cu(1)–N bond lengths are similar and unremarkable (ESI Table S5).† The apical and axial Cu–Cl bond lengths differ[51] with the equatorial Cu(1)–Cl(3) bond length of 2.250(1) Å being significantly shorter than that to the apical Cu(1)–Cl(2) bond [2.537(1) Å]. The Cu(II) centres in the complex are separated by 8.00 Å while the closest intermolecular separation of metal centres between neighbouring molecules is 7.29 Å.

Once again, two intramolecular C–H···Cl–Cu interactions between the equatorial Cl^- ligand and the aryl-H atoms H(21) and H(31) of the pyridine rings are present in the structure (Fig. 7); the respective distances are 2.79 and 2.77 Å (Table 3). Weak intermolecular C–H···Cl–M interactions involving the axial chloro ligand Cl(2) also occur: the shortest interaction corresponds to H(4)···Cl(2) (2.66 Å), with the C–H···Cl angle being 165°.

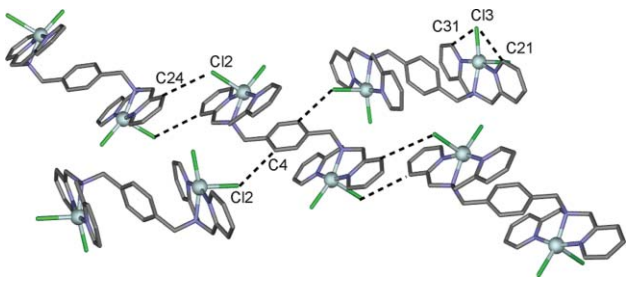

Fig. 7 Depiction of the intra- and intermolecular C–H···Cl-interactions in $[Cu_2(\mathbf{8})(Cl)_4]$. View along the b-axis.

It is noted that the structure of the trihydrate form $[Cu_2(\mathbf{8})(Cl)_4]\cdot 3H_2O$ of the present complex has been reported by Zhao *et al.*[15] This complex crystallises in the monoclinic system with the space group being C_2/c. Overall the structure is very similar to that of the above anhydrous complex.

$[Cu_2(9+H)(\mu\text{-}OCH_3)_2(H_2O)](ClO_4)_3\cdot C_4H_{10}O$. The final ligand in the series, 2,4,6-tris[di(2-picolyl)amino]triazine **9**, represents a new example of the relatively less common ligand category incorporating a trisubstituted triazine core.[16,52] Reaction of **9** in dichloromethane with $Cu(ClO_4)_2\cdot 6H_2O$ in methanol in a 1:3 molar ratio followed by slow diffusion of diethyl ether vapour into the solution yielded green-blue crystals. Despite the results of a visible spectrophotometric titration of **9** into an acetonitrile Cu(II) nitrate solution (concentration: 4.6 mM) clearly showing the stepwise formation of 1:1, 2:1 and 3:1 (M:L) complex species and presence

in the literature of an X-ray structure of a Cu(II) nitrate complex of **9** showing a 3:1 (M:L) stoichiometry,[16] a peak at $m/z = 1034$ in the ESI mass spectrum for a dinuclear $[2Cu + L + 2ClO_4 + Cl]^+$ ion (with the isotopic distribution for this ion in excellent agreement with the calculated pattern for a di-copper species) suggested the possibility that the present complex was a dinuclear species. The microanalysis of the solid complex was also in accord with such a formulation.

The X-ray structure of the above product confirmed the formation of a dinuclear complex of type $[Cu_2(\mathbf{9}+H)(\mu\text{-}OCH_3)_2(H_2O)](ClO_4)_3{\cdot}C_4H_{10}O$ in which one of the potential pyridine nitrogen coordination sites on **9** is protonated. The monoclinic unit cell contains four complex cations of type $[Cu_2(\mathbf{9}+H)(\mu\text{-}OCH_3)_2(H_2O)]^{3+}$, twelve perchlorate ions, and four ether molecules. The presence of basic amine sites on **9** presumably helps promote methoxide formation, with one amine site on each **9** being protonated in the process.

The Cu(II) ions in this dinuclear compound are bridged by two methoxides (see Fig. 8) with the Cu–Cu distance being 3.02 Å. The coordination spheres of Cu(1) and Cu(2) are not equivalent (Fig. 9); selected bond lengths and angles are listed in the ESI Table S6.† The N_3O_3-coordination sphere of Cu(2) is distorted octahedral, with the metal centre being bound to two pyridine nitrogen atoms from two dipic subunits, a tertiary nitrogen, N(9), from one of these, together with two methoxides and a water molecule. The Cu(1) centre is bound to two pyridine nitrogen atoms and two oxygen atoms from the methoxide bridges, with

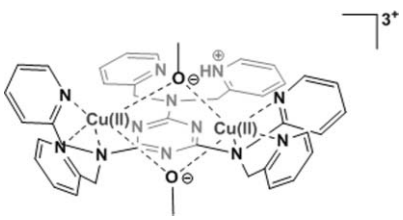

Fig. 8 Schematic representation of part of the coordination environment in $[Cu_2(\mathbf{9}+H)(\mu\text{-}OCH_3)_2(H_2O)]^{3+}$. For clarity, the coordinated water ligand is not shown.

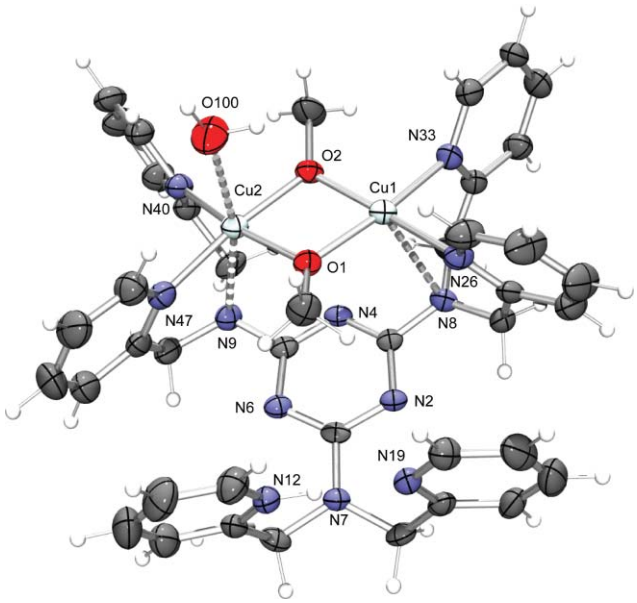

Fig. 9 ORTEP depiction of $[Cu_2(\mathbf{9}+H)(\mu\text{-}OCH_3)_2(H_2O)]^{3+}$ showing selected atom labels (50% thermal ellipsoids).

the corresponding bond lengths being comparable to those for Cu(2). The square pyramidal coordination sphere of Cu(1) is completed by a bond to the tertiary amine nitrogen N(8). As mentioned above, one pyridine nitrogen [N(12)] in the remaining dipic coordination unit of **8** is protonated, with the overall 3+ charge of the complex cation being compensated by three perchlorate counterions.

The Cu(1)–O(1)–Cu(2) and Cu(1)–O(2)–Cu(20 bridge angles in the four-membered ring are each 103° and comparable to literature values for the similar four-membered rings.[53]

A number of hydrogen bond interactions occur in $[Cu_2(\mathbf{9}+H)(\mu\text{-}OCH_3)_2(H_2O)]^{3+}$ and these are shown in Fig. 10 (see also ESI, Table S7).† A strong (charged) bifurcated hydrogen bond in the complex cation occurs between the protonated pyridyl nitrogen N(12) and the pyridine nitrogen atom N(19) together with the tertiary amine nitrogen N(7). The N(12)–N(19) distance is

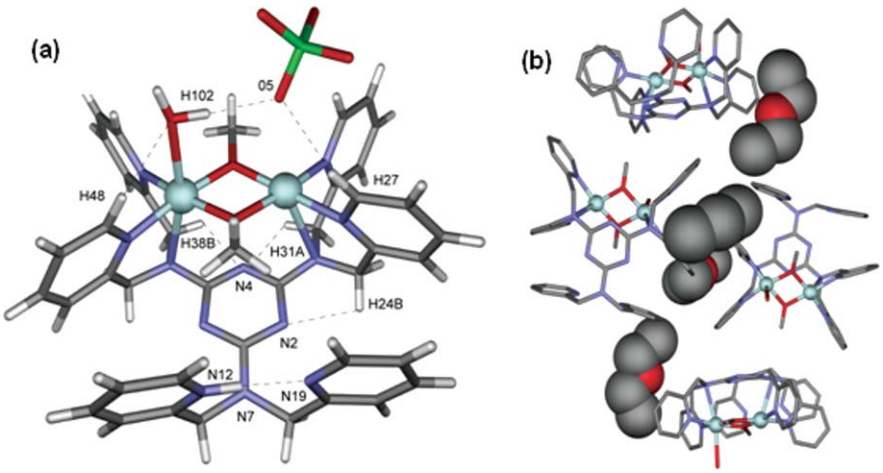

Fig. 10 (a). N^+–H···N, C–H···O, C–H···N and O–H···OCl interactions in the complex cation. (b). The unit cell of $[Cu_2(\mathbf{8}+H)(\mu\text{-}OCH_3)_2(H_2O)](ClO_4)_3{\cdot}C_4H_{10}O$ viewed along the *c*-axis. View of the diethyl ether molecules (space filling representation) in the unit cell; perchlorate ions and H-atoms, are omitted for clarity.

2.7 Å, with the N^+–H(12)···N(19) angle being 178°. C–H···N interactions in the cation involve the triazine nitrogen atoms N(2) and N(4) and a C–H···O interaction is also present involving the water oxygen atom and the perchlorate counter ion (see ESI, Table S8).† The respective intramolecular N^+–H···N, C–H···O, C–H···N interactions present in the complex cation are illustrated in Fig. 10. A number of π-stacking interactions are also present in the structure (see ESI, Tables S8 and S9).† Of particular interest is the observation that the 1,3,5-triazine moiety [N(2)–N(4)–N(6)] shows a weak π-interaction with the bridged Cu(II) [Cu(1)–O(2)–Cu(2)–O(1)] ring system, exemplified by short contacts between the copper centres and the triazine ring.

The unit cell viewed along the *c*-axis is given in Fig. 10(b) and shows the locations of the diethyl ether solvate molecules. The latter occupy 0.8 percent of the volume of the unit cell. A weak C–H···O-interaction is formed between the neighbouring methyl group and an ether oxygen [C(45)–H(45B)···O(3A): 3.38 Å, 169°, x, $1/2 - y$, $1/2 + z$].

Magnetic properties of complexes $[Cu(2)(\mu\text{-}Cl)]_2(PF_6)_2$ and $[Cu(3)(\mu\text{-}Cl)]_2(PF_6)_2\cdot 0.5H_2O$

The static magnetic susceptibility χ of the chloro-bridged complexes $[Cu(\mathbf{2})(\mu\text{-}Cl)]_2(PF_6)_2$ and $[Cu(\mathbf{3})(\mu\text{-}Cl)]_2(PF_6)_2\cdot 0.5H_2O$ has been studied at temperatures $T = 2$–300 K in a magnetic field $B =$ 1 T. The plot of the T-dependence of the inverse susceptibility $\chi^{-1}(T)$ is shown in Fig. 11.

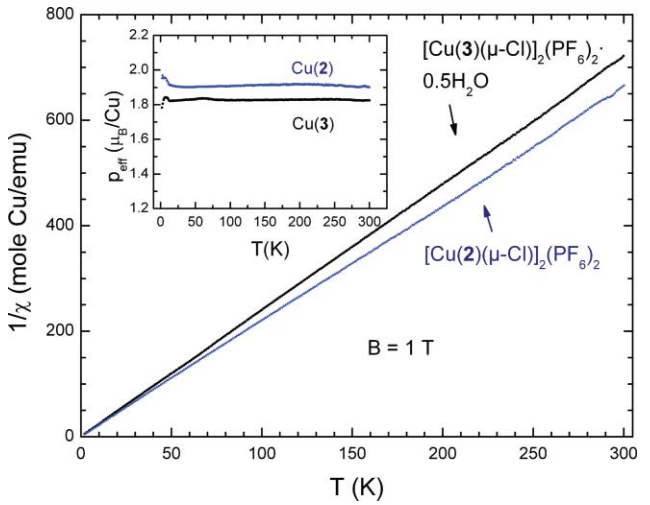

Fig. 11 Temperature dependence of the inverse static magnetic susceptibility χ^{-1} of complexes $[Cu(\mathbf{2})(\mu\text{-}Cl)]_2(PF_6)_2$ and $[Cu(\mathbf{3})(\mu\text{-}Cl)]_2(PF_6)_2\cdot 0.5H_2O$. A small temperature independent contribution χ_0 arising due to diamagnetism, Van-Vleck paramagnetism and instrumental effects has been subtracted from the raw data. Inset shows the effective magnetic moment calculated from the χ data (see the text).

In the whole temperature range χ^{-1} is linear in T following thus the Curie-Weiss law $\chi = C/(T+\theta)$ perfectly. Here C is the Curie constant and θ is the Curie-Weiss temperature. The fit yields $C = 0.454$ and 0.418 emuK/mole Cu for complexes $[Cu(\mathbf{2})(\mu\text{-}Cl)]_2(PF_6)_2$ and $[Cu(\mathbf{3})(\mu\text{-}Cl)]_2(PF_6)_2\cdot 0.5H_2O$, respectively. In both cases a small positive value of $\theta < 0.3$ K has been obtained from the fit, indicating a rather weak antiferromagnetic interaction between the Cu ions in these dimer complexes.

The magnitude of the effective magnetic moment p_{eff} which is related to $C \sim \chi T$ as $p_{eff} = (3Ck_B/N_A)^{1/2}$ is plotted in the inset of Fig. 11 as a function of temperature. It reveals an almost T-independent value of 1.91 and $1.83\mu_B$ for the first and second complex, respectively. Since in both cases the magnetic moment is associated with the spin 1/2 of the Cu(II) ion ($3d^9$, $S = 1/2$), in the absence of significant magnetic interactions the difference in the magnitude of the moment $p_{eff} = g[S(S+1)]^{1/2}\ \mu_B$ is related to the difference in the g-factors. From the above values of p_{eff} one obtains $g = 2.21$ and 2.11 for complexes $[Cu(\mathbf{2})(\mu\text{-}Cl)]_2(PF_6)_2$ and $[Cu(\mathbf{3})(\mu\text{-}Cl)]_2(PF_6)_2\cdot 0.5H_2O$, respectively. One should note, that since the g-factor of Cu(II) in a low symmetry ligand coordination is anisotropic, the above estimates represent a powder averaged value of the g-factor tensor.

The anisotropy of the g-factor can be demonstrated on the example of the powder ESR spectrum of $[Cu(\mathbf{3})(\mu\text{-}Cl)]_2(PF_6)_2\cdot 0.5H_2O$ (see Fig. 12). The asymmetric shape of the spectrum with a narrow high field peak and a broad low field part with a shoulder is characteristic for a uniaxial g-factor anisotropy with $g_\parallel > g_\perp$, where indexes ∥ and ⊥ denote the directions of the magnetic field parallel and perpendicular to the anisotropy axis. The low field shoulder and the high field peak are located roughly at resonance fields corresponding to $g_\parallel$ and $g_\perp$. A computer simulation of the powder spectrum is in good agreement with the experiment using the values of $g_\parallel = 2.19$ and $g_\perp = 2.06$ (Fig. 12). Indeed, a powder averaged value of $g = [(1/3)\ g_\parallel^2 + (2/3)\ g_\perp^2]^{1/2} =$ 2.10 is very close to the estimate from the static susceptibility data.

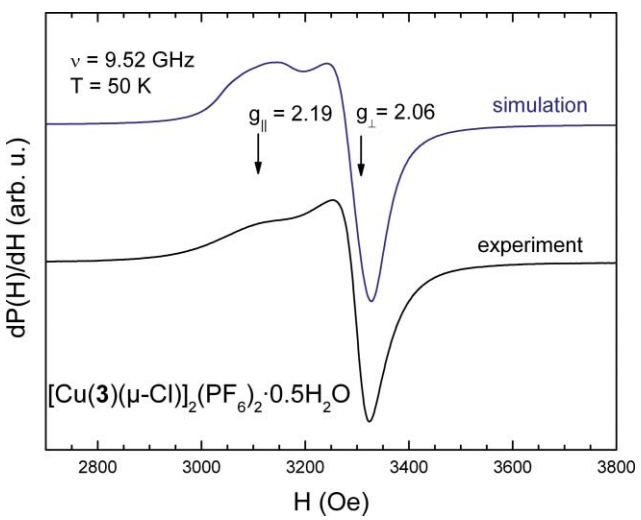

Fig. 12 ESR spectrum (field derivative of the absorbed power $dP(H)/dH$) of a powder sample of $[Cu(\mathbf{3})(\mu\text{-}Cl)]_2(PF_6)_2\cdot 0.5H_2O$ at a frequency of 9.52 GHz at $T = 50$ K. Low curve – experiment, upper curve – simulation. Arrows indicate the resonance fields corresponding to the principal g-factors $g_\parallel$ and $g_\perp$ (see the text for details).

Solvent extraction

A series of two-phase solvent extraction (water/chloroform) experiments involving the extraction of Cu(II) in the presence of **1**, **2**, **3**, **7**, **8** and **9** have been carried out. In each case the initial aqueous phase contained Cu(II) perchlorate at 1×10^{-4} M, sodium perchlorate at 5×10^{-3} M and was buffered at pH 7.2. The organic phase contained ligand at 1×10^{-3} M; namely, in

10-fold excess of the above Cu(II) ion concentration. Under these conditions the copper extraction by **1** was negligible (~2%) while a significant extraction was observed with each of the *N*-substituted derivatives **2** (34%), **3** (23%), **7** (28%), **8** (8%) and **9** (8%). At least in part, the behaviour of **2–9** appears likely to reflect the additional lipophilicities of the latter systems (relative to **1**) arising from the presence of the organic *N*-substituents. Interestingly, comparison of the results for the isomeric aryl-linked systems **7** (28%) and **8** (8%) indicates that substitution of the 1,3-aryl linkage in **7** with the 1,4-aryl link in **8** has a marked influence on extraction efficiency in this case.

Concluding remarks

The synthesis of the Cu(II) complexes of the extended series of substituted di(2-picolyl)amine derivatives **2–9** has been carried out and the crystal structures, magnetic properties and solvent extraction behaviour of selected complexes investigated. The series is characterised by a varied range of interesting coordination geometries and lattice architectures which in the case of $[Cu(\mathbf{6})(ClO_4)_2(H_2O)]\cdot 0.5H_2O$ includes a chain-like structure formed by unusual intermolecular π-interactions between metal bound perchlorate anions and the 'centre' aromatic rings of adjacent anthracenyl groups. The liquid–liquid ($H_2O/CHCl_3$) extraction experiments indicate that the presence of alkyl or aryl substituents on the secondary amine nitrogen of the parent di(2-picolyl)amine ligand results in enhanced extraction efficiencies for the systems investigated, undoubtedly reflecting the higher lipophilicities of the latter systems. Variable temperature magnetic studies of the dinuclear complexes of **2** and **3** confirm the presence of a weak antiferromagnetic interaction between the copper ions in each of these complexes.

Acknowledgements

We thank the Deutsche Forschungsgemeinschaft and the Australian Research Council for support. O. K. acknowledges the DFG for assistance under grants ME776/18-1 and 36RUS 17/20/06 and Prof. P. Metz for access to X-ray facilities at TU Dresden.

References

1 (*a*) E. C. Constable, *Chem. Soc. Rev.*, 2007, **36**, 246; (*b*) C. R. K. Glasson, L. F. Lindoy and G. V. Meehan, *Coord. Chem. Rev.*, 2008, **252**, 940.
2 A. Nielsen, S. Veltzé, A. D. Bond and C. J. McKenzie, *Polyhedron*, 2007, **26**, 1649.
3 C.-M. Liu, S. Gao, H.-Z. Kou, D.-Q. Zhang, H.-L. Sun and D.-B. Zhu, *Cryst. Growth Des.*, 2006, **6**, 94.
4 (*a*) K.-Y. Choi, H. Ryu, N. D. Sung and M. Suh, *J. Chem. Crystallogr.*, 2003, **33**, 947; (*b*) S. Ramakrishnan and M. Palaniandavar, *J. Chem. Sci.*, 2005, **117**, 179.
5 (*a*) K.-Y. Choi, B.-R. Kim and J. Ko, *J. Chem. Crystallogr.*, 2007, **37**, 847; (*b*) H.-W. Lee, H.-J. Seo, H.-J. Kim, S. K. Kang, J. Y. Heo and Y.-I. Kim, *Bull. Korean Chem. Soc.*, 2007, **28**, 855.
6 R. S. Rarig and J. Zubieta, *J. Solid State Chem.*, 2002, **167**, 370.
7 M. Palaniandavar, S. Mahadevan, M. Köckerling and G. Henkel, *J. Chem. Soc., Dalton Trans.*, 2000, 1151.
8 T. Murakami, Z. Orihashi, Y. Kikuchi, S. Igarashi and Y. Yukawa, *Inorg. Chim. Acta*, 2000, **303**, 148.
9 G.-S. Huang, J.-K. Lai, C.-H. Ueng and C.-C. Su, *Transition Met. Chem.*, 2000, **25**, 84.
10 T. Murakami, S. Hatakeyama, S. Igarashi and Y. Yukawa, *Inorg. Chim. Acta*, 2000, **310**, 96.
11 M. Palaniandavar, R. J. Butcher and A. W. Addison, *Inorg. Chem.*, 1996, **35**, 467.
12 G. Anderegg, E. Hubmann, G. Nitya and F. Wenk, *Helv. Chim. Acta*, 1977, **60**, 123.
13 O. Yamauchi, H. Benno and A. Nakahara, *Bull. Chem. Soc. Jpn.*, 1973, **46**, 3458.
14 (*a*) A. Kunishita, J. D. Scanion, H. Ishimaru, K. Honda, T. Ogura, M. Suzuki, C. J. Cramer and S. Itoh, *Inorg. Chem.*, 2008, **47**, 8222; (*b*) S. Turba, O. Walter, S. Schindler, L. P. Nielsen, A. Hazell, C. J. McKenzie, F. Lloret, J. Cano and M. Julve, *Inorg. Chem.*, 2008, **47**, 9612; (*c*) M. J. Belousoff, L. Tjioe, B. Graham and L. Spiccia, *Inorg. Chem.*, 2008, **47**, 8641; (*d*) Y. Sugai, S. Fujii, T. Fujimoto, S. Yano and Y. Mikata, *Dalton Trans.*, 2007, 3705; (*e*) M. Yano, M. Fujita, M. Miyake, M. Tatsumi, T. Yajima, O. Yamauchi, M. Oyana, K. Sato and T. Takuui, *Polyhedron*, 2007, **26**, 2174; (*f*) I. A. Koval, H. Akhideno, S. Tanase, C. Belle, C. Duboc, E. Saint-Aman, T. Patrick, M. Duncan, A. L. Spek, J.-L. Pierre and J. Reedijk, *New J. Chem.*, 2007, **31**, 512; (*g*) K.-Y. Choi, *J. Korean Chem. Soc.*, 2007, **51**, 31; (*h*) Y. Mikata, T. Fujimoto, Y. Sugai and S. Yano, *Eur. J. Inorg. Chem.*, 2007, 1143; (*i*) S. Foxon, J.-Y. Xu, S. Turba, M. Leibold, F. Hampel, F. W. Heinemann, O. Walter, C. Wuertele, M. Holthausen and S. Schindler, *Eur. J. Inorg. Chem.*, 2007, 429.
15 Y. Zhao, J. Zhu, W. He, Z. Yang, Y. Zhu, Y. Li, J. Zhang and Z. Guo, *Chem.–Eur. J.*, 2006, **12**, 6621.
16 P. U. Maheswari, B. Modec, A. Pevec, B. Kozlevčar, C. Massera, P. Gamez and J. Reedijk, *Inorg. Chem.*, 2006, **45**, 6637.
17 J. Kaizer, S. Goger, G. Speier, M. Regler and M. Giorgi, *Z. Kristallogr.*, 2006, **221**, 75.
18 S. Banthia and A. Samanta, *New J. Chem.*, 2005, **29**, 1007.
19 S. I. Kirin, P. Duebon, T. Weyhermueller, E. Bill and N. Metzler-Nolte, *Inorg. Chem.*, 2005, **44**, 5405.
20 S. Banthia and A. Samanta, *New J. Chem.*, 2005, **29**, 1007.
21 D. Rojas, A. M. Garcia, A. Vega, Y. Moreno, D. Venegas-Yazigi, M. T. Garland and J. Manzur, *Inorg. Chem.*, 2004, **43**, 6324.
22 N. Niklas, F. W. Heinemann, F. Hampel, T. Clark and R. Alsfasser, *Inorg. Chem.*, 2004, **43**, 4663.
23 B. Lucchese, K. J. Humphreys, D.-H. Lee, C. D. Incarvito, R. D. Sommer, A. L. Rheingold and K. D. Karlin, *Inorg. Chem.*, 2004, **43**, 5987.
24 J. Ackermann, F. Meyer and H. Pritzkow, *Inorg. Chim. Acta*, 2004, **357**, 3703.
25 F. Ugozzoli, C. Massera, A. M. M. Lanfredi, N. Marsich and A. Camus, *Inorg. Chim. Acta*, 2002, **340**, 97.
26 Z. He, D. C. Craig and S. B. Colbran, *J. Chem. Soc., Dalton Trans.*, 2002, 4224.
27 Y. Kani, S. Ohba, S. Ito and Y. Nishida, *Acta Crystallogr., Sect. C: Cryst. Struct. Commun.*, 2000, **56**, e195.
28 C. Walsdorff, S. Park, J. Kim, J. Heo, K.-M. Park, J. Oh and K. Kim, *J. Chem. Soc., Dalton Trans.*, 1999, 923.
29 D.-H. Lee, N. N. Murthy and K. D. Karlin, *Inorg. Chem.*, 1997, **36**, 5785.
30 (*a*) D. W. Gruenwedel, *Inorg. Chem.*, 1968, **7**, 495; (*b*) A. Almesaker, S. A. Bourne, G. Ramon, J. L. Scott and C. R. Strauss, *CrystEngComm*, 2007, **9**, 997.
31 M. Komiyama, S. Kina, K. Matsumura, J. Sumaoka, S. Tobey, V. M. Lynch and E. Anslyn, *J. Am. Chem. Soc.*, 2002, **124**, 13731.
32 K. J. Humphreys, K. D. Karlin and S. E. Rokita, *J. Am. Chem. Soc.*, 2002, **124**, 6009.
33 S. T. Frey, H. H. J. Sun, N. N. Murthy and K. D. Karlin, *Inorg. Chim. Acta*, 1996, **242**, 329.
34 B. Antonioli, D. J. Bray, J. K. Clegg, K. A. Jolliffe, K. Gloe, K. Gloe, L. F. Lindoy, P. J. Steel, C. J. Sumby and M. Wenzel, *Polyhedron*, 2008, **27**, 2889.
35 (*a*) B. Antonioli, D. J. Bray, J. K. Clegg, K. Gloe, K. Gloe, O. Kataeva, L. F. Lindoy, J. C. McMurtrie, P. J. Steel, C. J. Sumby and M. Wenzel, *Dalton Trans.*, 2006, 4783; (*b*) J. K. Clegg, B. Antonioli, D. J. Bray, K. Gloe, K. Gloe, H. Heßke and L. F. Lindoy, *CrystEngComm*, 2006, 748.
36 D. R. V. Staverena and N. Metzler-Nolte, *Chem. Commun.*, 2002, 1406.
37 A. Ojida, Y. Mito-oka, M.-A. Inoue and I. Hamachi, *J. Am. Chem. Soc.*, 2002, **124**, 6256.
38 S. Kawahara and T. Uchimaru, *Eur. J. Inorg. Chem.*, 2001, 2437.
39 P. de Hoog, P. Gamez, W. L. Driessen and J. Reedijk, *Tetrahedron Lett.*, 2002, **43**, 6783.

40 Nonius BV, Delft, The Netherlands, 1998.
41 A. J. M. Duisenberg, *J. Appl. Crystallogr.*, 1992, **25**, 92.
42 A. J. M. Duisenberg, L. M. J. Kroon-Batenburg and A. M. M. Schreurs, *J. Appl. Crystallogr.*, 2003, **36**, 220.
43 *Bruker, SMART, SAINT and XPREP*, Bruker Analytical X-ray Instruments Inc., Madison, Wisconsin, USA, 1995.
44 G. M. Sheldrick, *Acta Crystallogr., Sect. A: Found. Crystallogr.*, 1990, **46**, 467.
45 G. M. Sheldrick, *SADABS: Empirical Absorption and Correction Software*, University of Göttingen, Institut für Anorganische Chemie der Universität, Tammanstrasse 4, D-3400 Göttingen, Germany, 1999-2003.
46 G. M. Sheldrick, *SHELX-97: Programs for Crystal Structure Analysis*, University of Göttingen, Institut für Anorganische Chemie der Universität, Tammanstrasse 4, D-3400 Göttingen, Germany, 1997.
47 A. W. Addison, T. N. Rao, J. Reedijk, J. van Rijn and G. C. Verschoor, *J. Chem. Soc., Dalton Trans.*, 1984, 1349.
48 (*a*) W. J. Belcher, M. Fabre, T. Farhan and J. W. Steed, *Org. Biomol. Chem.*, 2006, **4**, 781; (*b*) D. L. Reger, R. F. Semeniuc and M. D. Smith, *J. Chem. Soc., Dalton Trans.*, 2002, 476; (*c*) C. Janiak, *J. Chem. Soc., Dalton Trans.*, 2000, 3885.
49 R. S. Rowland and R. Taylor, *J. Phys. Chem.*, 1996, **100**, 7384.
50 R. Ahuja and A. G. Samuelson, *CrystEngComm*, 2003, **5**, 395.
51 See, for example: D. C. Craig, S. B. Colbran and P. V. Bernhardt, *Dalton Trans.*, 2004, 778.
52 (*a*) See for example: P. De Hoog, P. Gamez, M. Lüken, O. Roubeau, B. Krebs and J. Reedijk, *Inorg. Chim. Acta*, 2004, **357**, 213; (*b*) S. Demenshko, S. Dechert and F. Meyer, *J. Am. Chem. Soc.*, 2004, **126**, 4508; (*c*) J. Pang, Y. Tao, S. Freiberg, X.-P. Yang, M. D'Iorio and S. Wang, *J. Mater. Chem.*, 2002, **12**, 206; (*d*) A. M. Garcia, D. M. Bassani, J.-M. Lehn, G. Baum and D. Fenske, *Chem.–Eur. J.*, 1999, **5**, 1234; (*e*) E. I. Lerner and S. J. Lippard, *Inorg. Chem.*, 1977, **16**, 1546; (*f*) F. H. Case and E. Koft, *J. Am. Chem. Soc.*, 1959, **81**, 905.
53 T. Ishida, K. Yanagi and T. Nogami, *Inorg. Chem.*, 2005, **44**, 7307.